

Which physics for full-wavefield seismic inversion?

M Warner, J Morgan, A Umpleby, I Stekl, L Guasch (Imperial College London)

Introduction

Full waveform seismic inversion (FWI) in three dimensions has been used principally in one of two modes: (1) using low-frequency, long-offset, refracted arrivals to obtain high-resolution macro-velocity models for subsequent depth migration, and (2) using short-offset near-normal-incidence reflections to obtain high-wavenumber velocity or impedance models that can be directly interpreted. In current commercial practice, both approaches simplify the physics of wave propagation, typically they emphasise only some parts of the total recorded wavefield, and they seek to match only some of the properties of those wavefields. These approximations and compromises are made both to reduce the total compute cost of FWI, and to circumvent the necessity to invert for multiple parameters that may be ill constrained by the available data.

In this paper, we examine the consequences of these practical compromises by generating synthetic seismic data using a realistic 3D model, and then invert these data using different approximations to the physics of wave propagation in the forward and inverse modelling. We also invert using different portions of the data, and examine the effects of matching data amplitudes locally and globally.

Methodology

The synthetic data to be inverted were generated using a fully three-dimensional model based loosely upon the well-understood 2D Marmousi model. The original model was extended, and variably stretched and sheared in the third dimension such that dip lines appear qualitatively similar to Marmousi, and strike lines show a mix of asymmetric synforms and antiforms. We used this model to generate 3D time-domain seismic data:

- using acoustic and elastic wave equations,
- using isotropic and anisotropic acoustic models with various types of anisotropy,
- with and without anelastic attenuation,
- with and without a model of density that is independent of the velocity model,
- with and without a fixed V_p/V_s ratio,
- with and without free-surface ghosts and multiples.

The model contains a homogeneous, isotropic, fluid, non-attenuating "water" layer at the top. We have generated both single and multi-component data; in this study we report the results only of inverting data from single-component pressure sources and single-component pressure receivers located within the water layer. The data to be inverted were generated using a single line of 90 sources along a 9-km dip line through the centre of the model recorded on a dense fixed swath of receivers that covered the 9×5 km horizontal extent of the 3D model. The data were modelled using a source with useful energy up to about 32 Hz; they were inverted within the bandwidth 2 to 15 Hz using a fixed parameterisation for all the datasets, and a starting model that was almost cycle skipped at the longest offsets at 2 Hz.

Results

Figures 1 (a) & (b) show shot records, along the line of section shown in Figure 2a, generated using isotropic, non-attenuative acoustic and elastic forward modelling respectively. Comparing the two figures, shows that the kinematics of early arrivals in both records are essentially identical, but their amplitude behaviour is quite different. It can also be seen that there is much-more late, slow energy visible in the elastic record than in the acoustic one. These arrivals mostly represent doubly converted p-s-p waves of various kinds; there are no actual shear arrivals in the data because the receivers are within a fluid layer. Close inspection shows that the data are also reasonably well matched, both kinematically and dynamically, for the shortest-offset reflections. The records suggest that acoustic inversion of elastic data will give sensible results provided that the inversion is restricted towards early arrivals or very-short offsets, and that it does not attempt to fit amplitude behaviour in detail.

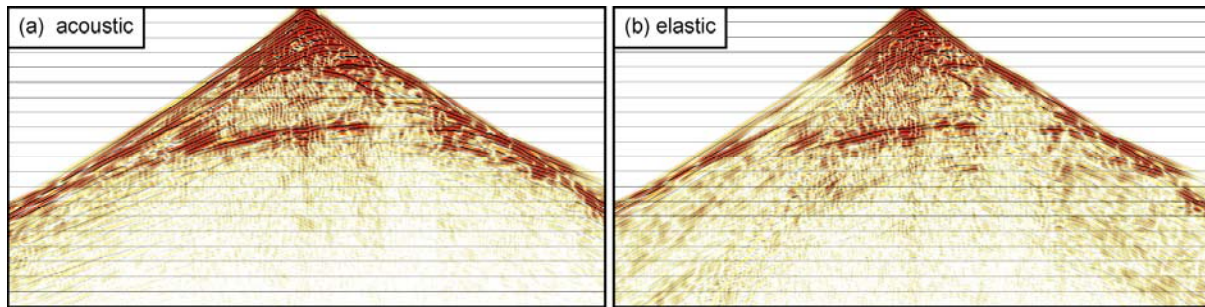


Figure 1 A shot record from the 3D model generated using (a) acoustic, and (b) elastic modelling. Total time 4000 ms, spread length 9000m, one line is shown from an array of receivers 9×5 km.

Figure 2(b) shows the result of applying an acoustic inversion to the acoustic data, using a FWI scheme that inverts fully for amplitudes and that uses all available offsets and times. Where there is good coverage of the subsurface by the recorded data, the structure is well-recovered down to scale-lengths of about half the seismic wavelength at the maximum frequency used in the inversion. The accuracy of the recovered model decays where there is poorer data coverage towards the bottom and outer edges of the model. This is the type of inversion that is often shown in synthetic studies; in our view however it generates results that cannot be realistically obtained from field data.

Figure 2(c) also shows acoustic inversion of acoustic data. In this case however, the seismic data have been weighted towards early refracted arrivals, and the local RMS amplitudes of both the input and predicted data have been normalised to a single value. Such an inversion scheme predominantly inverts the kinematics of the early arrivals, together with the local amplitude behaviour within each individual trace at early times; it pays no attention to amplitude variation between traces, and it pays little attention to the systematic decay of amplitude with time. In our view, this approach produces results that are more representative of the real performance of FWI on field data, especially when it is applied in order to obtain velocity models for subsequent depth imaging.

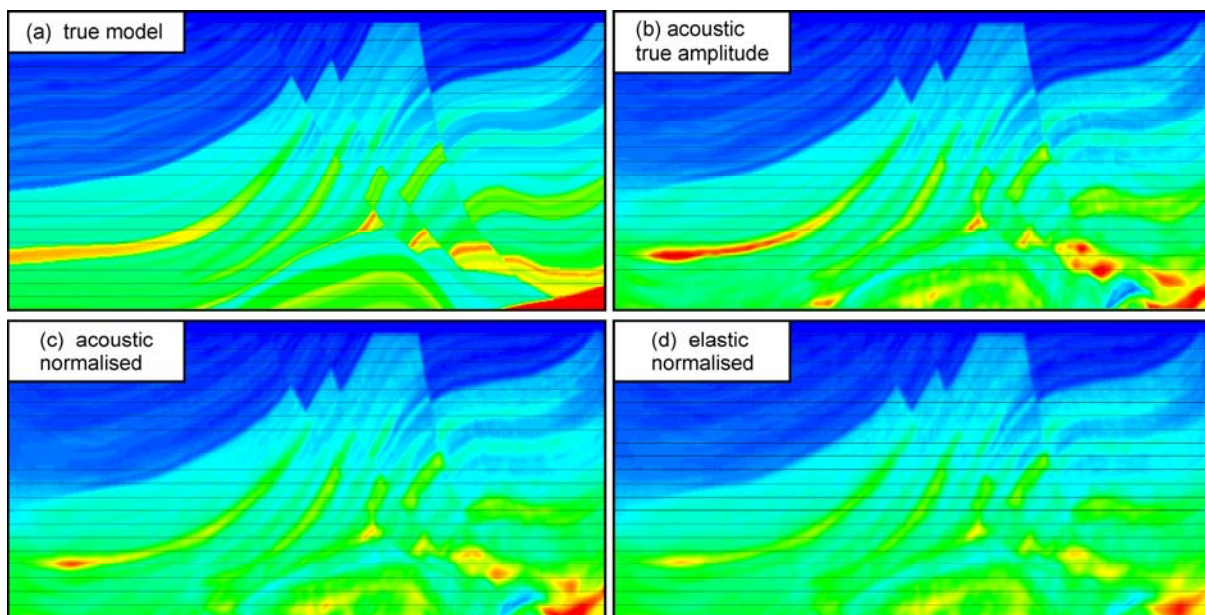


Figure 2 Vertical slices through the original and FWI-recovered velocity models. In each case, the inversion used an acoustic algorithm. (b) & (c) invert acoustic data, (d) inverts elastic data. In (c) and (d), the input data are amplitude-normalised and weighted towards early arrivals.

Comparison of Figures 2(b) & (c) shows the uplift that amplitudes and later reflected energy can theoretically bring to FWI. In those areas of the subsurface where there is full data coverage, the figures are similar, but Figure 2(b) is always somewhat sharper. The largest differences between the figures are seen in those parts of the model where there is less than full sub-surface coverage, and this difference increases as the coverage worsens. The principal contribution of amplitudes and reflections is thus seen to be the sharpening of reflecting boundaries, and improved accuracy and resolution in those parts of the model where the data coverage is incomplete.

The real world of course is elastic, not acoustic. Figure 2(d) therefore provides a result that is more representative of field data; it shows the result of inverting elastic data using an acoustic algorithm identical to that used to generate Figure 2(c). These two figures are remarkably similar – the principal differences are in those parts of the model that have limited data coverage. In contrast, if we had inverted these elastic data with an acoustic algorithm using a true-amplitude approach similar to that used for Figure 2(b), the resulting model would have shown many artefacts and inaccuracies.

In summary, Figures 1 and 2 demonstrate that acoustic inversion of elastic data can provide accurate, well resolved, artefact-free, p-wave velocity images. They also show that the uplift that amplitudes and reflections can in principle bring to wide-angle FWI are unlikely to be realised on field data using acoustic inversion algorithms; in such cases either amplitudes and reflected arrivals should be suppressed, or a fully elastic inversion algorithm should be used.

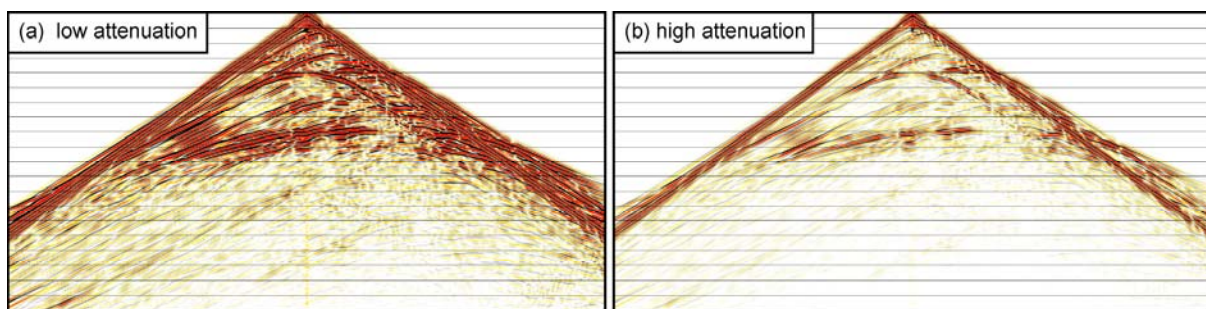


Figure 3 Shot records from models with (a) low, and (b) high attenuation.

As well as being elastic, the real world also involves attenuation. Figure 3 shows a shot record from two models that have different degrees of anelastic attenuation; the models are otherwise identical. In Figure 3(a), $Q = 1000$ everywhere below the water layer; in 3(b), a heterogeneous low- Q varies between 65 and 450, increasing with depth and velocity. The absolute amplitude behaviour, and the decay of amplitude with time and offset, is quite different in the two records. Close inspection shows also that attenuation produces small but significant effects on the kinematics of all arrivals as well as changing their dynamics – attenuation causes dispersion which delays energy within the wavelet.

Inverting these data using the correct attenuation model produces results that match closely those shown in Figure 2(b). However, inverting the data from Figure 3(b) using true amplitudes and late arrivals, without including attenuation into the inversion modelling, produces the poor result shown in Figure 4(a). This model contains artefacts, and it is strongly attenuated with depth. More subtly, the average velocities are too low in the deeper part of the recovered model because the kinematics of the data are affected by attenuation, and this remains uncorrected during the non-attenuative FWI.

Since field data are always affected by attenuation – both anelastic and because of sub-wavelength-scale scattering – these effects must be properly compensated before or during the inversion if either lateral variation of amplitudes or local decay of amplitude with time is to be included within the FWI algorithm. In practice this compensation is difficult to achieve accurately, and so in many circumstances it is desirable to neglect amplitude behaviour during FWI of field data. Some caution is required however even in this case because attenuation will tend to lower the effective velocity with increasing depth – indeed most methods of velocity analysis will suffer from similar problems.

In full-wavefield inversion, it is difficult to separate the effects of velocity and density. Consequently FWI typically proceeds by assuming a fixed relationship between these parameters. If the inversion is driven more strongly by the kinematics than the dynamics, and if the assumed velocity-density relationship is broadly correct, then this has few practical consequences. However, if the inversion is driven to fit amplitudes, and especially to fit the amplitudes of reflections, and if density and velocity are not related in a known way, then significant artefacts can appear in the results.

Figure 4(b) shows a result of inverting a dataset generated using a complicated density model. In this model, some velocity boundaries had no significant change in acoustic impedance across them, some density boundaries did not have any associated velocity change, and the relationship between density and velocity was significantly different in different lithological units. Figure 4(b) should look similar to Figure 2(b) – the inversion algorithm used was the same, and full account was taken of all amplitudes and all arrivals. Clearly the recovered model contains many artefacts, and if we did not know the real model, then it would be difficult to identify these, either from the model or from the data.

In contrast, if these variable-density data are inverted using a scheme similar to that used in Figure 2(c), then the resulting inverted velocity model is similar to 2(c), and the artefacts are strongly suppressed. Similarly, if we invert the data using the correct density model, we do recover a model similar to that shown in Figure 2(b). For field data, we generally know rather little about the true density model, and it is difficult to invert for it. We are led again to the same conclusion – amplitudes and reflections will generally not be helpful in wide-angle FWI of field data unless great care is taken to deal with them properly.

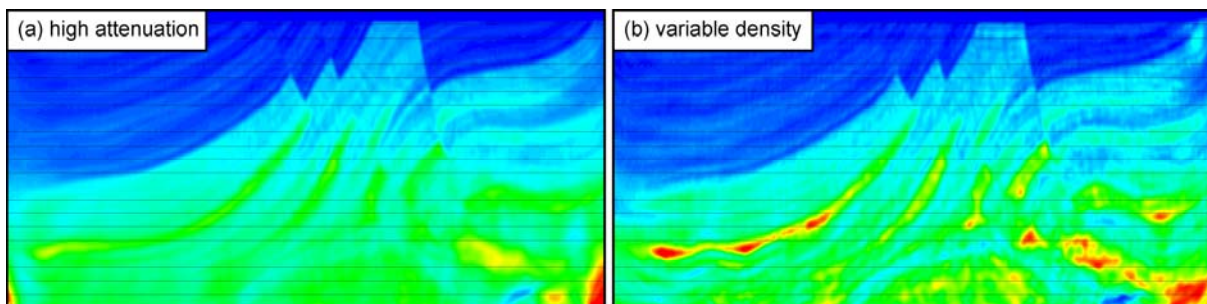


Figure 4 FWI-recovered models using true-amplitude inversion applied to data with (a) significant but unknown attenuation, and (b) significant but unknown density variation.

We have also looked at the effects of anisotropy, of variable V_p/V_s , and 2D vs 3D inversion, and of different FWI strategies. From these comprehensive tests, we are able to prioritise the importance of different effects in wide-angle FWI. Our conclusions are these:

- If the intent is to use FWI to generate p-wave velocity models for depth migration, then 3D FWI is required, 2D is not adequate, the kinematic effects of anisotropy must be included in the FWI when they are present in the field data, and it will normally be counter-productive to try to fit amplitudes, reflections or other late arrivals.
- If the intent is to use FWI to generate fully-quantitative models of physical properties at high-resolution at the reservoir, then amplitudes must be included, but they must be modelled correctly. The order of importance is usually 3D (rather than 2D), then p-wave anisotropy, then attenuation, then density and elastic effects are of similar importance, then s-wave and attenuation anisotropy.
- It is not sensible to use elastic inversion in 2D – the effects of moving from 2D to 3D are much larger than those of moving from acoustic to elastic modelling, and it is not sensible to use elastic inversion in 3D unless it also correctly incorporates at least the kinematics of p-wave anisotropy.